

# Crystal structure and Hirshfeld surface analysis of pinaverium bromide dihydrate

Dezhen Chen <sup>1</sup>, Wangting Zhou,<sup>1</sup> Yujing Wei,<sup>1</sup> Chenghan Zhuang,<sup>2</sup> Yazheng He,<sup>2</sup> Xiaoli Li,<sup>2</sup> Kaibo Li,<sup>2</sup> Zhaoxia Zhang,<sup>1,(a)</sup> and Guoqing Zhang<sup>1</sup>

<sup>1</sup>School of Materials Science and Engineering, Zhejiang Sci-Tech University, Hangzhou 310018, People's Republic of China

<sup>2</sup>Zhejiang Apeloa Jiayuan Pharmaceutical Co., Ltd, Dongyang 322118, People's Republic of China

(Received 16 March 2024; accepted 28 August 2024)

In the present study, we have discovered and identified a new crystalline form of pinaverium bromide, pinaverium bromide dihydrate ( $C_{26}H_{41}BrNO_4 \cdot Br \cdot 2H_2O$ ), whose single crystals can be obtained by recrystallization from a mixture of water and acetonitrile at room temperature. The obtained crystals were characterized by X-ray single-crystal diffraction, and their crystal structure was also solved based on X-ray single-crystal diffraction data. The results show that the final pinaverium bromide dihydrate model contains an asymmetric unit of one pinaverium bromide ( $C_{26}H_{41}Br_2NO_4$ ) molecule and two water molecules that combine with the bromine ion through O–H...O and O–H...Br hydrogen bonds. Then, the adjacent pinaverium bromide dihydrates are linked by O–H...O, O–H...Br, and C–H...O hydrogen bonds. On the other hand, the experimentally obtained X-ray powder diffraction pattern is in good agreement with the simulated diffraction pattern from their single-crystal data, confirming the correctness of the crystal structure. Hirshfeld surface analysis was employed to understand and visualize the packing patterns, indicating that the H...H interaction is the main acting force in the crystal stacking of pinaverium bromide dihydrate.

© The Author(s), 2024. Published by Cambridge University Press on behalf of International Centre for Diffraction Data.

[doi:10.1017/S0885715624000423]

Keywords: pinaverium bromide, antispasmodic agent, dihydrate, crystal structure, Hirshfeld surface

## I. INTRODUCTION

Pinaverium bromide (4-[(2-bromo-4,5-dimethoxyphenyl)methyl]-4-[2-[2-(6,6-dimethyl-bicyclo[3,1,1]-hept-2-yl)ethoxy]ethyl]morpholinium bromide,  $C_{26}H_{41}Br_2NO_4$ ) is a muscletropic spasmolytic drug virtually devoid of anticholinergic action (Christen, 1990; Annaházi et al., 2014). As a calcium antagonist, it inhibits the flux of calcium into intestinal smooth muscle cells. It exerts this effect by blocking the L-type voltage-dependent calcium channels (the most common type of voltage-operated calcium channel in the intestinal smooth muscle) at the level of the  $\alpha_1$ -subunit by blocking voltage-dependent calcium channels within the intestinal smooth muscle cells (Christen, 1990; Froguel et al., 1990; Dai et al., 2003; Bor et al., 2021). As a typical crystalline drug, so far the crystal structure of pinaverium bromide has not been reported, and only X-ray powder diffraction patterns of its polycrystalline forms were collected and reported (Mendoza et al., 2021).

Here, a new crystalline form, pinaverium bromide dihydrate ( $C_{26}H_{41}BrNO_4 \cdot Br \cdot 2H_2O$ ) as shown in Figure 1, was discovered and its single crystals were also obtained by solution volatilization, and then its crystal structure was characterized and solved by X-ray single-crystal diffractometry. Furthermore, the intermolecular forces and stacking patterns of pinaverium bromide dihydrate were analyzed using the Hirshfeld surface analysis.

Meanwhile, the polycrystalline products of pinaverium bromide were also prepared by grinding the single crystals and characterized using X-ray powder diffractometry. X-ray powder diffraction (XPRD) is the most effective characterization tool for identifying polycrystalline forms of drugs. The XPRD pattern can also be used to verify the accuracy of the single-crystal data.

## II. EXPERIMENTAL

### A. Preparation and testing of single crystals

The pinaverium bromide raw material was provided by Zhejiang Apeloa Medical Technology Co., Ltd (Jinhua, China). Analytical grade acetonitrile (ACN) was purchased

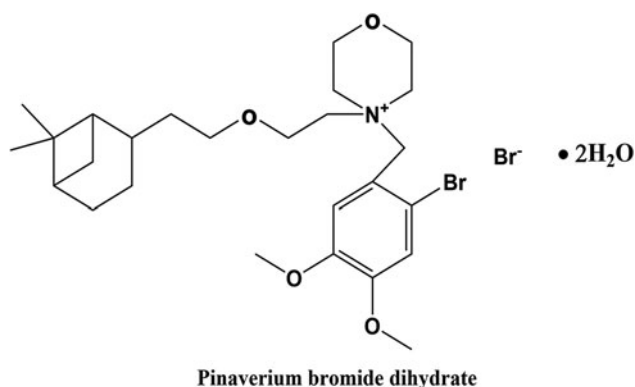


Figure 1. The pinaverium bromide dihydrate.

<sup>a)</sup> Author to whom correspondence should be addressed. Electronic mail: zhangzx@zstu.edu.cn

TABLE I. Experimental details.

Crystal data	
Chemical formula	$C_{26}H_{41}BrNO_4 \cdot Br \cdot 2H_2O$
$M_r$	627.45
Crystal system, space group	Triclinic, $P\bar{1}$
Temperature (K)	296
$a, b, c$ (Å)	7.3128(4), 13.5547(7), 15.4049(8)
$\alpha, \beta, \gamma$ (°)	81.568(2), 82.425(2), 85.881(2)
$V$ (Å <sup>3</sup> )	1495.14(14)
$Z$	2
Radiation type	Mo $K\alpha$ ( $\lambda = 0.71073$ )
$\mu$ (mm <sup>-1</sup> )	2.75
Crystal size (mm)	0.15 × 0.05 × 0.03
Data collection	
Diffractometer	Bruker APEX-II CCD
$T_{min}, T_{max}$	0.607, 0.746
No. of measured, independent, and observed [ $I > 2\sigma(I)$ ] reflections	65 718, 6610, 5072
$R_{int}$	0.041
$(\sin \theta/\lambda)_{max}$ (Å <sup>-1</sup> )	0.642
Refinement	
$R[F^2 > 2\sigma(F^2)], wR(F^2), S$	0.060, 0.200, 1.05
No. of reflections	6610
No. of parameters	340
No. of restraints	125
H-atom treatment	H-atom parameters constrained
$\Delta\rho_{max}, \Delta\rho_{min}$ (e Å <sup>-3</sup> )	0.64, -0.62

For the single-crystal structure: triclinic,  $P\bar{1}$ ,  $Z = 2$ . Experiments were carried out at 296 K with Mo  $K\alpha$  radiation using a Bruker APEX-II CCD diffractometer. Absorption was corrected for by multi-scan methods (SADABS; Bruker, 2016). Computer programs: APEX2 (Bruker, 2016), SAINT (Bruker, 2016), OLEX2 (Dolomanov et al., 2009), SHELXT (Sheldrick, 2015a), SHELXL2014 (Sheldrick, 2015b).

from Hangzhou ShuangLin Chemical Reagent Co., Ltd (Hangzhou, China), and the purified water was obtained using a Millipore Milli-Q Purification System. All chemical reagents were used without further purification.

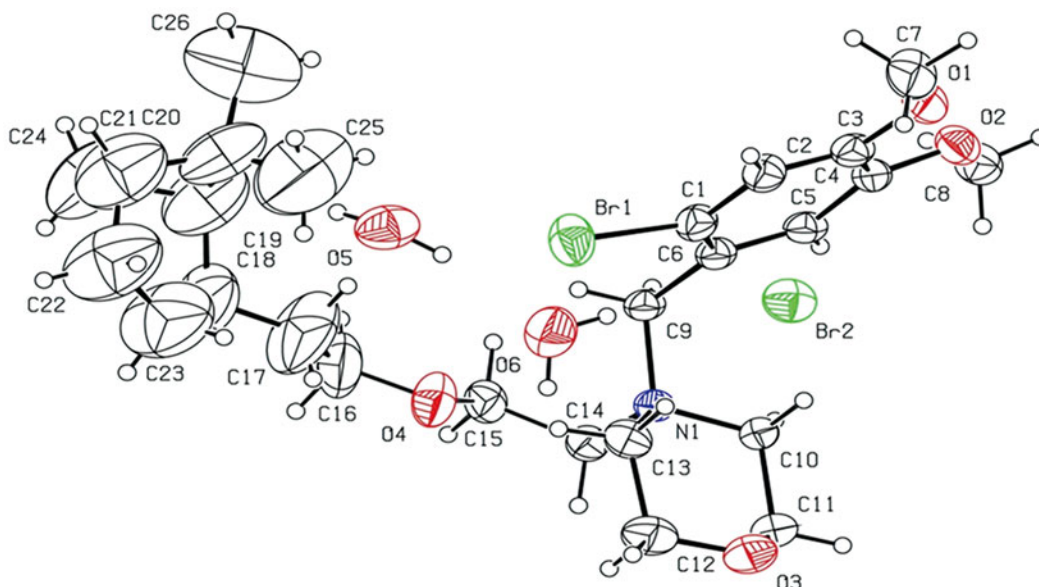


Figure 2. The asymmetric unit of pinaverium bromide dihydrate, with displacement ellipsoids drawn at the 40% probability level and H atoms represented by spheres of arbitrary size.

In a typical experiment, pinaverium bromide (0.2 g) and ACN/H<sub>2</sub>O (1/1, v/v, 10 ml) were mixed in a beaker under stirring until the solution became clear and then covered with a PVC film with a few pores. After slowly evaporating at room temperature, colorless lumpy single crystals appeared in the solution. Subsequently, a suitable single crystal was selected for measurement by single-crystal methods and the determination of the crystal structure.

A suitable crystal (0.15 × 0.05 × 0.03 mm<sup>3</sup>) was selected and mounted on a glass fiber support on a Bruker APEX-II CCD diffractometer. The crystal was kept at a steady  $T = 296$  K during data collection.

## B. Refinement

Crystal data, data collection, and structure refinement details for pinaverium bromide dihydrate are summarized in Table I. All H atoms were placed geometrically and treated with riding constraints. The  $U_{iso}(H)$  values of all CH<sub>2</sub> and CH groups are fixed to 1.2 times the  $U_{eq}$  value of the attached C atom. CH<sub>3</sub> groups are idealized as freely rotating groups, and their  $U_{iso}(H)$  values are fixed to 1.5 times the  $U_{eq}$  value of the attached C atom, and for H atoms on water molecules, their  $U_{iso}(H)$  values are also fixed to 1.5 times the  $U_{eq}$  value of the attached oxygen atom.

In the determined crystal structure, the middle portion of pibromium dihydrate exhibited disorder, and the refinement of the disordered group was made anisotropically. The disorder was modeled as two site occupancies with occupancy factors of 0.668(19) and 0.332(19) for the C15/O4 and C15A/O4A groups, respectively.

## C. X-ray powder diffraction

The sample was carefully mounted on a flat plate to ensure uniform exposure to the X-ray source. X-ray powder diffraction patterns were collected using a D8 Advance diffractometer (Bruker, Germany), which is equipped with a Cu  $K\alpha_1$

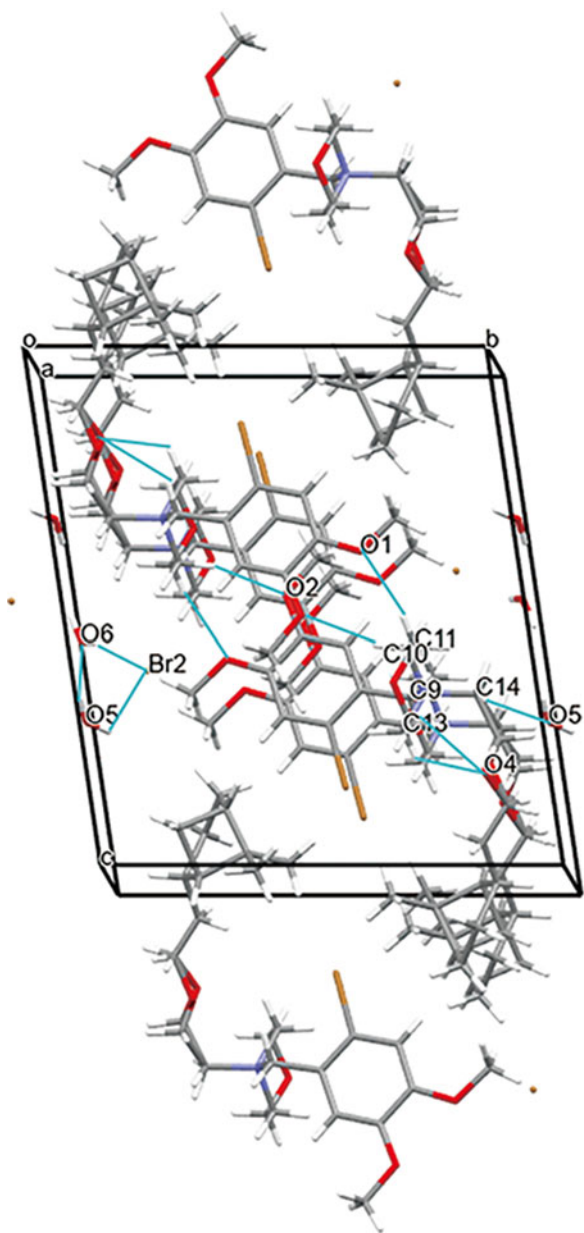


Figure 3. The single-crystal cell of pinaverium bromide dihydrate is viewed along the *a*-axis direction. The blue line represents the hydrogen bonding. And viewed along the *b*-axis and *c*-axis direction are given in Figures 8–9 (supplementary material).

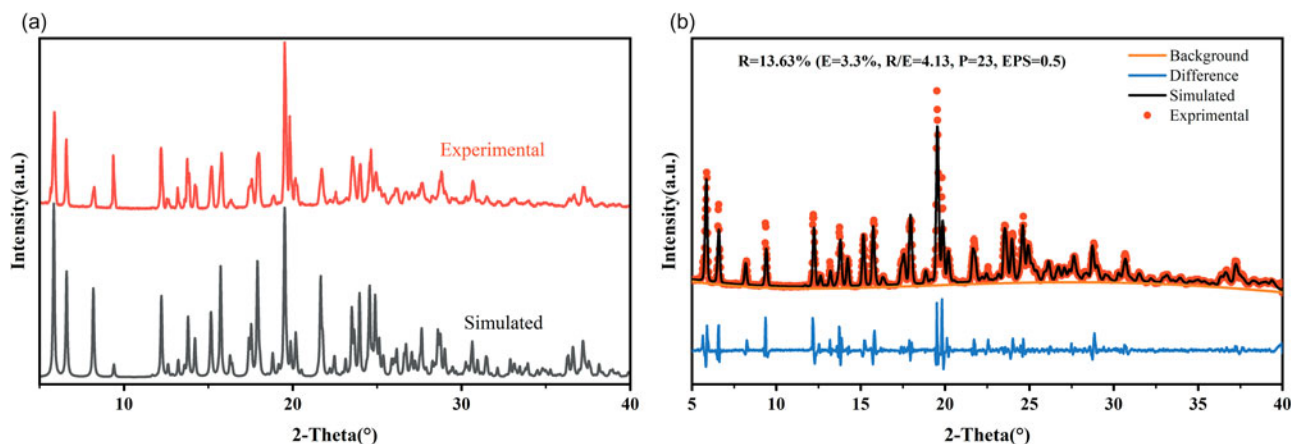


Figure 4. (a) X-ray powder diffraction pattern of pinaverium bromide dihydrate and (b) Whole Pattern Fitting and Rietveld refinement results.

TABLE II. Hydrogen bond geometry ( $\text{\AA}$ ,  $^\circ$ ) for pinaverium bromide dihydrate

	D–H	H...A	D...A	D–H...A
C9–H9B...O4	0.97	2.60	3.205(14)	120.9
C10–H10B...O2 <sup>i</sup>	0.97	2.46	3.313(5)	147.1
C11–H11B...O1 <sup>i</sup>	0.97	2.64	3.337(6)	129.4
C13–H13A...O4	0.97	2.36	3.053(11)	127.9
C14–H14A...O5 <sup>ii</sup>	0.97	2.46	3.379(6)	157.2
O5–H5B...O6	0.86	2.03	2.869(6)	164.1
O6–H6A...Br2 <sup>iii</sup>	0.85	2.53	3.382(5)	176.0
O6–H6B...Br2	0.85	2.68	3.353(4)	136.7

Symmetry code: (i)  $-x+2, -y+1, -z+1$ ; (ii)  $x-1, y, z$ ; (iii)  $-x+2, -y+2, -z+1$ .

X-ray ( $\lambda = 1.5406 \text{ \AA}$ ). The measurements were conducted using a fixed slit of 0.6 mm and a solar slit of  $2.5^\circ$  to optimize the beam divergence and intensity. The X-ray tube was operated at a voltage of 40 kV and a current of 40 mA. A LYNXEYE- XE-T detector was employed to collect XRD data over a  $2\theta$  range from  $5^\circ$  to  $40^\circ$ , with a step size of  $0.02^\circ$  and a total of 1750 data points were recorded.

#### D. Hirshfeld surface analysis

Hirshfeld surface analysis and the related two-dimensional (2D) fingerprint plots were calculated using CrystalExplorer (Jayatilaka et al., 2006; Spackman et al., 2021) from the structure input file in the CIF format.

### III. RESULTS AND DISCUSSION

#### A. Crystal and molecular structure

During recrystallization from a mixture of ACN and water, water molecules were incorporated into the lattice to form pinaverium bromide dihydrate with a stoichiometric ratio of 1:2. Table I shows the crystallographic data, data collection, and structural refinement details of pivibromide dihydrate, i.e., crystal system, space group, and cell metric.

The single-crystal X-ray diffraction data show that the pinaverium bromide dihydrate crystallizes in the triclinic space group  $P\bar{1}$ . An asymmetric unit includes one pinaverium bromide molecule and two water molecules, where as one pinaverium molecule contains a cation and an anion.

The view of the asymmetric unit is shown in Figure 2. From the crystal stacking, the molecules are laminated along the *a*-axis, and the benzene ring C1–C6 is located in a planar position and interconnected with the morpholine group through the methylene group, which is basically in the same plane as the benzene ring, and the torsion angle between them is only 1.1(5)° for C4–C5–C6–C1. In addition, the torsion angle between the morpholine group and the methylene group is 90.9(4)° for C5–C6–C9–N1.

Hydrogen bonding plays a crucial role in the crystal formation process. Pinaverium bromide dihydrate exhibits a unique hydrogen bonding as well as molecular stacking pattern. As shown in Figure 3 (red for oxygen atoms, purple for nitrogen atoms, white for hydrogen atoms, gray for carbon atoms, and dark yellow for bromine atoms), the molecules can stack stably through intramolecular and intermolecular hydrogen bonding interactions. Firstly, pinaverium bromide and water molecules are hydrogen bonded by groups of O5–H5B···O6 hydrogen bonds as well as O6–H6···Br2, and the pinaverium bromide cations in adjacent molecules are connected through C10–H10B···O2<sup>i</sup> and C11–H11B···O1<sup>i</sup>, while Br<sup>−</sup> is connected to a water molecule through O6–H6A···Br2<sup>iii</sup>

and O6–H6B···Br2 hydrogen bonds. At the same time, the cation also forms a C14–H14A···O5<sup>ii</sup> hydrogen bond with the nearest water molecule, which further stabilizes the crystal structure of pinaverium bromide dihydrate. Hydrogen bond geometry (Å, °) for pinaverium bromide dihydrate is listed in Table II. See supplementary material for the details.

## B. X-ray powder diffraction analysis

After knowing the atomic coordinates in the cell, the experimental X-ray diffraction pattern of pinaverium bromide dihydrate was simulated using Mercury software (Macrae et al., 2019) and compared with the experimentally obtained XRPD pattern. Figure 4(a) shows good agreement between the experimental diffraction pattern and the simulated pattern from the single-crystal structure. It can be concluded that the crystal structure of the powder crystal samples is highly consistent with that of a single crystal and shows high purity and homogeneous structure. It is worth noting that some diffraction planes, especially those with *h*=0 such as (0 1 1) and (0 3 2), show lower intensity compared

TABLE III. X-ray powder diffraction data of pinaverium bromide dihydrate before and after whole Pattern Fitting and Rietveld refinement.

$2\theta_{\text{obs}}$ (°)	$2\theta_{\text{cal}}$ (°)	$\Delta 2\theta$ (°)	<i>h</i>	<i>k</i>	<i>l</i>	$d_{\text{obs}}$ (Å)	Height	$I_{\text{obs}}$ (%)	Area	FWHM
5.875	5.885	0.010	0	0	1	15.0434	5229	59.1	43 776	0.145
6.574	6.577	0.003	0	1	0	13.4453	3652	41.3	21 409	0.102
8.238	8.239	0.001	0	1	1	10.7325	1161	13.1	9900	0.148
9.368	9.356	−0.012	0	−1	1	9.4408	2950	33.3	17 311	0.102
12.197	12.194	−0.003	1	0	0	7.2565	3470	39.2	26 204	0.131
12.544	12.535	−0.009	0	1	2	7.0562	493	5.6	4416	0.155
13.179	13.175	−0.004	0	2	0	6.7178	1007	11.4	5864	0.101
13.747	13.733	−0.014	1	1	1	6.4413	2779	31.4	21 451	0.134
14.216	14.228	0.012	−1	0	1	6.2299	1282	14.5	11 407	0.154
15.193	15.181	−0.012	0	−2	1	5.8316	2364	26.7	21 460	0.157
15.786	15.782	−0.004	−1	−1	1	5.6138	3174	35.9	30 028	0.164
16.337	16.316	−0.021	0	2	2	5.4258	439	5	4594	0.181
17.578	14.581	0.003	0	0	3	5.0452	1562	17.7	24 620	0.273
17.987	17.990	0.003	−1	0	2	4.9315	3130	35.4	35 274	0.195
18.866	18.872	0.006	0	−2	2	4.7037	494	5.6	4223	0.148
19.538	19.522	−0.016	−1	−2	1	4.5434	8848	100	75 038	0.147
19.825	19.815	−0.010	0	3	0	4.4781	4605	52	36 470	0.137
20.15	20.125	−0.025	1	0	3	4.4067	1393	15.7	16 314	0.203
21.72	21.698	−0.022	0	3	2	4.0916	2051	23.2	24 155	0.204
22.539	22.564	0.025	1	3	1	3.9448	551	6.2	5054	0.159
23.555	23.529	−0.026	0	−2	3	3.7769	2611	29.5	35 533	0.236
24.002	23.980	−0.022	−1	3	0	3.7075	2142	24.2	17 808	0.144
24.635	24.648	0.013	2	0	1	3.6137	2854	32.2	34 087	0.207
24.941	24.951	0.010	2	1	1	3.57	1703	19.3	42 283	0.43
25.43	25.416	−0.014	−1	2	3	3.5025	528	6	5414	0.178
26.104	26.202	0.098	−2	0	1	3.4135	813	9.2	13 870	0.296
26.737	26.779	0.042	−2	−1	1	3.3342	619	7	7985	0.224
27.064	27.063	−0.001	1	−1	4	3.2946	571	6.5	15 921	0.483
27.673	27.677	0.004	0	4	2	3.2234	1123	12.7	22 789	0.352
28.286	28.234	−0.052	1	4	1	3.155	330	3.7	6696	0.352
28.834	28.846	0.012	1	4	0	3.0962	1708	19.3	32 181	0.327
29.059	29.025	−0.034	2	−2	1	3.0728	560	6.3	21 648	0.67
30.266	30.239	−0.027	1	1	5	2.9529	350	4	7364	0.365
30.692	30.680	−0.012	0	−4	2	2.913	1240	14	19 249	0.269
31.508	31.493	−0.015	−1	4	2	2.8393	394	4.5	4565	0.201
33.14	33.104	−0.036	1	−4	2	2.7032	377	4.3	10 345	0.475
36.401	36.403	0.002	−1	5	1	2.4681	386	4.4	7773	0.349
36.667	36.653	−0.014	2	4	3	2.4508	596	6.7	10 607	0.308
37.277	37.208	−0.069	2	−3	3	2.4121	1014	11.5	16 861	0.288
37.625	37.619	−0.006	1	4	5	2.3906	365	4.1	5779	0.275

to the fitted data, indicating the existence of preferred orientations.

In order to obtain more accurate results, this paper used the Whole Pattern Fitting and Rietveld Refinement features of MDI Jade 9 software (MDI, 2019) to perform Rietveld refinement of the powder XRD pattern and then compares it with the simulated XRD data from the single crystals. As shown in Figure 4(b), the Whole Pattern Fitting and Rietveld refinement, including the background, specimen displacement, lattice constants, overall intensity scale factor, peak width, peak symmetry parameters, skewness factor, absorption correction, and atomic structure, was carried out successfully. In addition, it is clear that the crystals mainly grow along the  $\langle 1\ 0\ 0 \rangle$  axis; here, the orientation coefficient of the  $(1\ 0\ 0)$  diffraction plane is calculated to be 0.75. The residuals of the final fit,  $R = 13.63\%$ , is less than 15%, which is an acceptable error range. The relevant data for refinement, including  $2\theta_{\text{obs}}$ ,  $2\theta_{\text{cal}}$ ,  $\Delta 2\theta$ ,  $d$ ,  $I$ , height, area, and full width at half maximum (FWHM), are listed in Table III.

### C. Hirshfeld surface analysis

The stacking properties of crystals are explored by using the Hirshfeld surface analysis in the CrystalExplorer program. This method allows the identification and analysis of close contacts occurring between molecules in a crystal. Figures 5 displays the Hirshfeld surfaces of the pinaverium bromide dihydrate,  $d_i$  and  $d_e$  denote the distance from the surface to the nearest atom inside or outside to the surface (Sundareswaran and Karuppanan, 2020), respectively, and  $d_{\text{norm}}$  is the surface map that depicts the individual hydrogen bonding interactions on the  $d_{\text{norm}}$  surface, respectively. In addition, the strong hydrogen bonding contacts are depicted

as large circular depressions (dark red) on the  $d_{\text{norm}}$  surface. Other contacts, i.e., those that are weaker and longer than the hydrogen bonds, are depicted as small dots and very lightly colored regions (Spackman and McKinnon, 2002).

Figure 5 represents the Hirshfeld surfaces of pinaverium bromide dihydrate mapped over  $d_{\text{norm}}$ ,  $d_i$ ,  $d_e$ , shape index, and curvedness. In the map, the larger red dots indicate stronger hydrogen bonding interactions between molecules. It can be seen from Figure 5 that the Br atoms in the pinaverium ammonium bromide dihydrate molecule and the O–H in the water molecule form strong (O–H $\cdots$ Br) interactions with the O–H and Br atoms in the neighboring molecules. The shape index represents the bumps (blue) and hollows (red) present in the system, and the curvedness shows that the structure contains almost flat surface areas (green) with sharp edges (blue).

Different molecular interactions have different two-dimensional fingerprints, and the two-dimensional fingerprints are very sensitive to the environment in which the molecules are located, so they can be used to reflect the modes of interaction between molecules within different crystalline forms and the contribution range of each mode of interaction to the overall action (Nikpour et al., 2009). The two-dimensional fingerprint plots of the Hirshfeld surface of pinaverium bromide dihydrate and the percentage contribution of various modes of action to Hirshfeld are shown in Figures 6 and 7.

It can be seen from Figures 6 and 7 that there are seven main intermolecular interactions of pinaverium bromide dihydrate, among which the H $\cdots$ H interactions between the methyl and methylene groups of adjacent molecules are distributed in the middle region of the fingerprint profile, which is the most dominant mode with the largest contribution of 59.4% to the Hirshfeld surface, followed by the intermolecular O $\cdots$ H and Br $\cdots$ H interactions, which contributed 11.4%. In fact, according to the  $d_{\text{norm}}$  diagram, Br $\cdots$ H interactions are mainly from

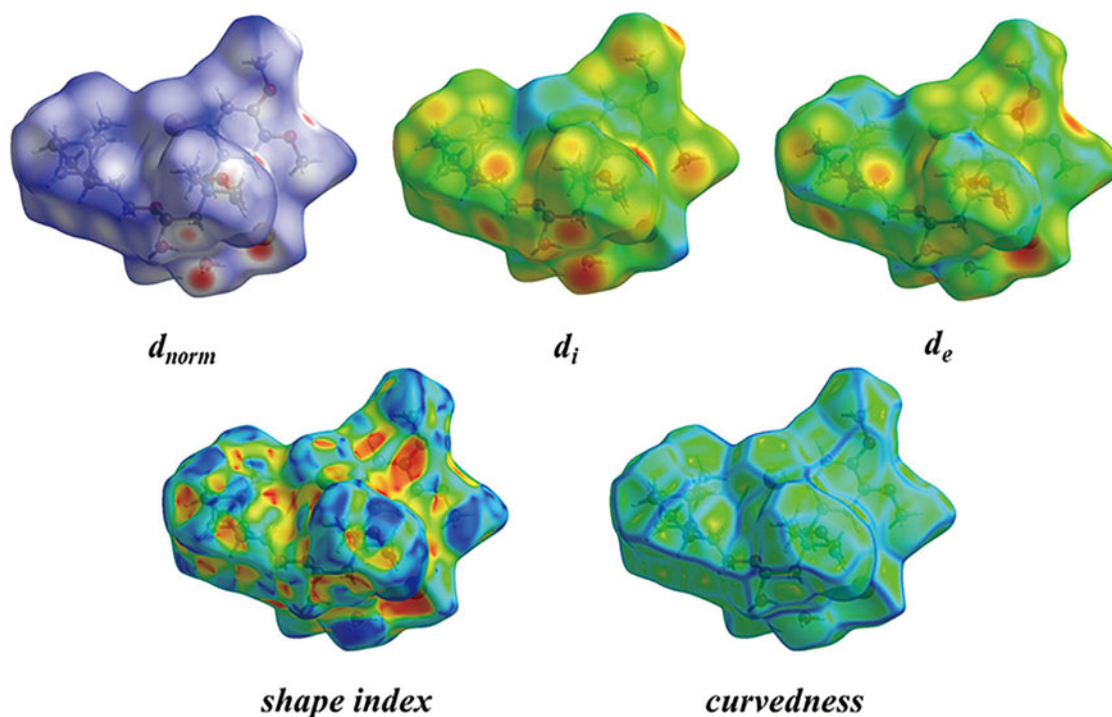


Figure 5. Hirshfeld surface analysis of pinaverium bromide dihydrate.

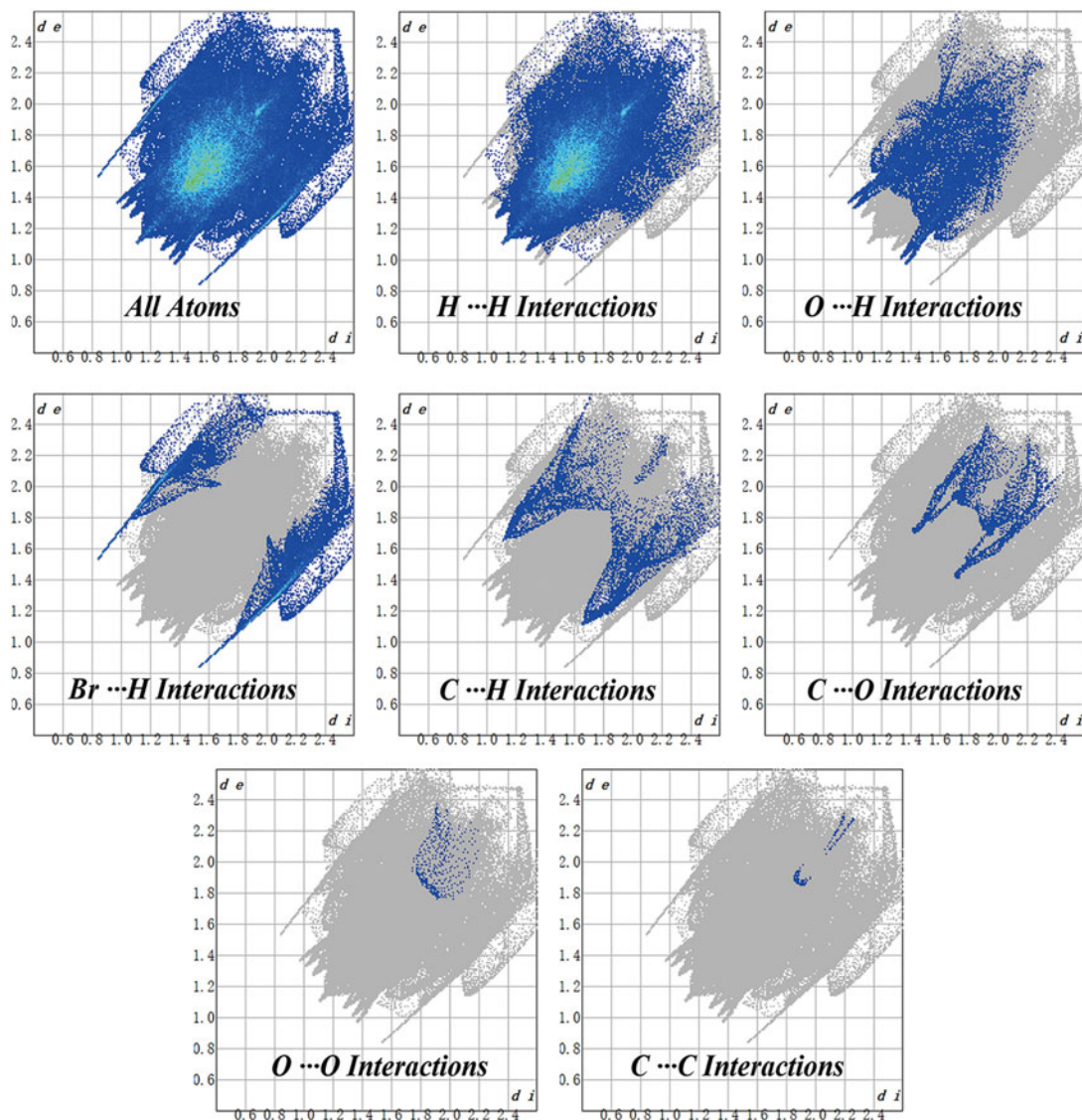


Figure 6. The 2D fingerprint plots (atom-atom interactions) of the Hirshfeld surface of pinaverium bromide dihydrate.

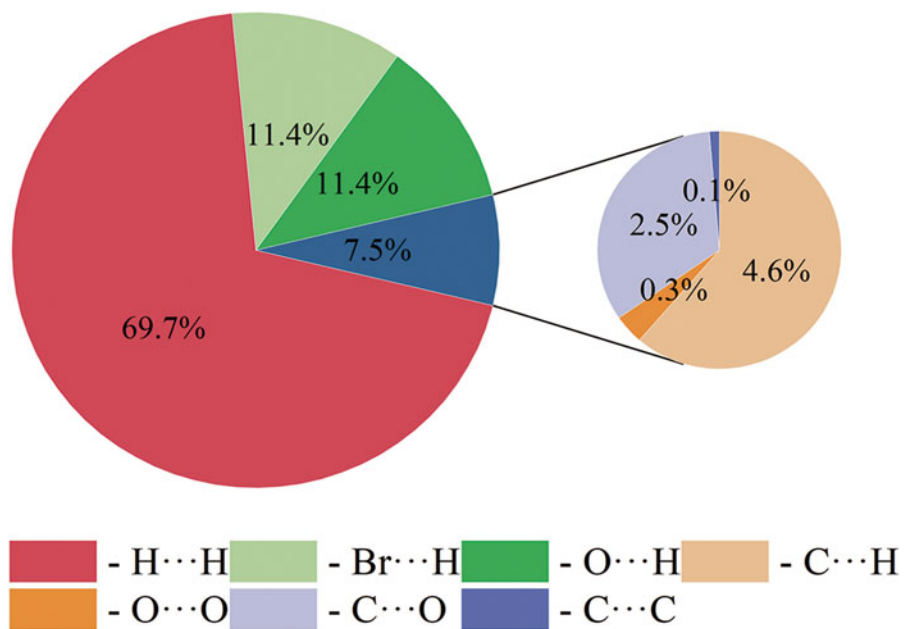


Figure 7. Relative contributions of various intermolecular interactions to the Hirshfeld surface area in pinaverium bromide dihydrate.

the C–H...Br van der Waals forces between H and Br atoms and O–H...Br hydrogen bonding forces; meanwhile, O...H interactions can be attributed to the van der Waals forces between O and H atoms and the intermolecular C–H...O hydrogen bonding forces, indicating that hydrogen bonding plays a key role in the intermolecular interaction.

The corresponding interaction distances based on Hirshfeld analysis are calculated to be 2.897 Å (C5–H5...Br2), 2.869 Å (C10–H10A...Br2), 2.593 Å (O6–H6...Br2), 1.913 Å (O5–H5B...O6), and 2.597 Å (C14–H14C...O6). It is obvious that the interaction distance is related to the force strength of the hydrogen bond. The stronger the hydrogen bond is, the shorter the interaction distance is.

#### IV. CONCLUSION

In this paper, single crystals of pinaverium bromide dihydrate were prepared from the ACN/water system by slow volatilization and its crystal structure was determined by single-crystal X-ray diffraction analysis. The results show that the pinaverium bromide dihydrate molecules crystallize in the triclinic space group  $P\bar{1}$ , with one cell containing two pinaverium bromide dihydrate molecules arranged along the *a*-axis. The dihydrate molecules are connected by four intramolecular and four intermolecular hydrogen bonds when the crystals are stacked. Particularly, H...H, Br...H, and O...H interactions play an important role in the self-assembly process of stabilized pinaverium bromide dihydrate crystals. In addition, the XRPD pattern simulated from the single-crystal structure of pinaverium bromide dihydrate is in good agreement with the experimentally obtained powder pattern, implying the correctness of the crystal structure model solved from the single-crystal data.

#### SUPPLEMENTARY MATERIAL

The supplementary material for this article can be found at <https://doi.org/10.1017/S0885715624000423>.

#### DEPOSITED DATA

Deposited crystallographic information is available by request at [pdj@icdd.com](mailto:pdj@icdd.com).

#### FUNDING STATEMENT

Funding for this research was provided by the National Natural Science Foundation of China (contract No. 22075252).

#### CONFLICT OF INTEREST

The authors have no conflict of interest to declare.

#### REFERENCES

- Annaházi, A., R. Róka, A. Rosztóczy, and T. Wittmann. 2014. "Role of Antispasmodics in the Treatment of Irritable Bowel Syndrome." *World Journal of Gastroenterology* 20 (20): 6031–43.
- Bor, S., P. Leher, A. Chalbaud, and J. Tack. 2021. "Efficacy of Pinaverium Bromide in the Treatment of Irritable Bowel Syndrome: A Systematic Review and Meta-Analysis." *Therapeutic Advances in Gastroenterology* 14: 1–12.
- Bruker 2016. *Program name(s)*. Madison, WI, Bruker AXS.
- Christen, M. O. 1990. "Action of Pinaverium Bromide, a Calcium-Antagonist, on Gastrointestinal Motility Disorders." *General Pharmacology* 21 (6): 821–5.
- Dai, Y., J. X. Liu, J. X. Li, and Y. F. Xu. 2003. "Effect of Pinaverium Bromide on Stress-Induced Colonic Smooth Muscle Contractility Disorder in Rats." *World Journal of Gastroenterology* 9 (3): 557–61.
- Dolomanov, O. V., L. J. Bourhis, R. J. Gildea, J. A. K. Howard, and H. Puschmann. 2009. "OLEX2: A Complete Structure Solution, Refinement and Analysis Program." *Journal of Applied Crystallography* 42: 339–41.
- Froguel, E., S. Chaussade, H. Roche, M. Fallet, D. Couturier, and J. Guerre. 1990. "Effects of an Intestinal Smooth Muscle Calcium Channel Blocker (Pinaverium Bromide) on Colonic Transit Time in Humans." *Neurogastroenterology & Motility* 2 (3): 176–9.
- Jayatilaka, D., S. K. Wolff, D. J. Grimwood, J. J. McKinnon, and M. A. Spackman. 2006. "Crystalexplorer: A Tool for Displaying Hirshfeld Surfaces and Visualising Intermolecular Interactions in Molecular Crystals." *Acta Crystallographica Section A: Foundations and Advances* 62: s90.
- Macrae, C. F., I. Sovago, S. J. Cottrell, P. T. A. Galek, P. McCabe, E. Pidcock, M. Platings, G. P. Shields, J. S. Stevens, M. Towler, and P. A. Wood. 2019. "Mercury 4.0: From Visualization to Analysis, Design and Prediction." *Journal Applied Crystallography* 53: 226–35.
- MDI. 2019. *JADE Version 9.6*. Livermore, CA, Materials Data.
- Mendoza, J. H. Q., A. P. Aparicio, and J. A. Henao. 2021. "Powder Diffraction Data and Preliminary Spectroscopic and Thermal Characterization of Pinaverium Bromide, a Drug Used for Functional Gastrointestinal Disorders." *Powder Diffraction* 36 (1): 20–4.
- Nikpour, M., M. Mirzaei, Y. G. Chen, A. A. Kaju, and M. Bakavoli. 2009. "Contribution of Intermolecular Interactions to Constructing Supramolecular Architecture: Synthesis, Structure and Hirshfeld Surface Analysis of a New Hybrid of Polyoxomolybdate and ((1H-tetrazole-5-yl) Methyl) Morpholine." *Inorganic Chemistry Communications* 12 (9): 879–882.
- Sheldrick, G. M. 2015a. "SHELXT – Integrated Space-Group and crystal-Structure Determination." *Acta Crystallographica Section A Foundations and Advances* 71: 3–8.
- Sheldrick, G. M. 2015b. "Crystal Structure Refinement with SHELXL." *Acta Crystallographica Section C Structural Chemistry* 71: 3–8.
- Spackman, M. A., and J. J. McKinnon. 2002. "Fingerprinting Intermolecular Interactions in Molecular Crystals." *CrystEngComm* 4 (66): 378–92.
- Spackman, P. R., M. J. Turner, J. J. McKinnon, S. K. Wolff, D. J. Grimwood, D. Jayatilaka, and M. A. Spackman. 2021. "Crystalexplorer: A Program for Hirshfeld Surface Analysis, Visualization and Quantitative Analysis of Molecular Crystals." *Journal of Applied Crystallography* 54: 1006–1011.
- Sundareswaran, S., and S. Karuppannan. 2020. "Hirshfeld Surface Analysis of Stable and Metastable Polymorphs of Vanillin." *Crystal Research and Technology* 55 (11): 2000083.